Acta Biomaterialia 8 (2012) 1037–1047

Contents lists available at SciVerse ScienceDirect

Acta Biomaterialia

journal homepage: www.elsevier.com/locate/actabiomat

Engineering hydrophobin DewA to generate surfaces that enhance adhesion of human but not bacterial cells

Stephane Boeuf [a], Tanja Throm [b], Beatrice Gutt [b], Timo Strunk [c], Marc Hoffmann [a], Elisabeth Seebach [a], Leonie Mühlberg [a], Jan Brocher [a], Tobias Gotterbarm [a], Wolfgang Wenzel [c], Reinhard Fischer [b], Wiltrud Richter [a,*]

[a] Research Centre for Experimental Orthopaedics, Orthopaedic University Hospital Heidelberg, Schlierbacher Landstrasse 200a, 69118 Heidelberg, Germany
[b] Department of Microbiology, Institute for Applied Biosciences, Karlsruhe Institute of Technology, Hertzstraße 16, 76187 Karlsruhe, Germany
[c] Institute of Nanotechnology, Karlsruhe Institute of Technology, Hermann-von-Helmholtz-Platz 1, 76344 Eggenstein-Leopoldshafen, Germany

ARTICLE INFO

Article history:
Received 22 June 2011
Received in revised form 15 November 2011
Accepted 21 November 2011
Available online 2 December 2011

Keywords:
Hydrophobin
Mesenchymal stem cell
Bacterial infection
Implant coating
Orthopaedic implants

ABSTRACT

Hydrophobins are fungal proteins with the ability to form immunologically inert membranes of high stability, properties that makes them attractive candidates for orthopaedic implant coatings. Cell adhesion on the surface of such implants is necessary for better integration with the neighbouring tissue; however, hydrophobin surfaces do not mediate cell adhesion. The aim of this project was therefore to investigate whether the class I hydrophobin DewA from *Aspergillus nidulans* can be functionalized for use on orthopaedic implant surfaces. DewA variants bearing either one RGD sequence or the laminin globular domain LG3 binding motif were engineered. The surfaces of both variants showed significantly increased adhesion of mesenchymal stem cells (MSCs), osteoblasts, fibroblasts and chondrocytes; in contrast, the insertion of binding motifs RGD and LG3 in DewA did not increase *Staphylococcus aureus* adhesion to the hydrophobin surfaces. Proliferation of MSCs and their osteogenic, chondrogenic and adipogenic differentiation potential were not affected on these surfaces. The engineered surfaces therefore enhanced MSC adhesion without interfering with their functionality or leading to increased risk of bacterial infection.

1. Introduction

Hydrophobins are fungal proteins with the ability to form amphipathic membranes by self-assembling at hydrophilic–hydrophobic interfaces. If these membranes are formed on a solid surface, they can convert the hydrophobicity of this surface. A Teflon surface, for example, can be made hydrophilic by the addition of a hydrophobin layer [1]. The assembly of class I hydrophobins is associated with the formation of amyloid fibrils [2], and assembled class I hydrophobins bind strongly to their supports, resisting harsh treatments such as boiling using water or detergents [3].

Hydrophobins are found on fungal spores and the tissues of fruiting bodies that have been exposed to air [4,5]. The hydrophobin coating on spores creates an affinity with hydrophobic surfaces, which facilitates their dispersal in the air. In addition to these biophysical properties, hydrophobins have also been shown to be important in the interaction between spores and their host post-inhalation. The hydrophobin RodA, from *Aspergillus fumigatus*, is immunologically inert. It does not induce maturation of dendritic cells and alveolar macrophages or activate helper T-cells, and it is proposed to function as a shield, preventing immune response to spores [6]. Hydrophobins therefore represent non-immunogenic proteins with the capacity to change the property of surfaces via a stable coating of thin layers. These various properties suggest that hydrophobins may be interesting compounds for use in medical applications [3].

Materials with surfaces that permit good integration with human tissue are in high demand for tissue engineering and medical implants. For prosthetic implants in particular, osseointegration that guarantees stability and prevents subsequent loosening from bone is highly desirable. One means of promoting this integration is to use implants with surfaces on which progenitor cells can attach and differentiate to form new bone [7]. Mesenchymal stem cells (MSCs) are present in the bone marrow and represent the most important cell population, with the ability to regenerate mesenchymal tissues [8]. The adhesion of MSCs to implant surfaces under conditions that maintain their osteogenic differentiation potential could therefore promote the integration of an implant. On the other hand, adhesion of bacterial cells is undesirable on implant surfaces. The infection of prosthetic joints with virulent microorganisms such as *Staphylococcus aureus* is a devastating complication with high morbidity [9]. Bacterial adhesion is a first step leading to biofilm formation and inflammation, which may

* Corresponding author. Tel.: +49 6221 96 92 53; fax: +49 6221 96 92 88.
E-mail address: wiltrud.richter@med.uni-heidelberg.de (W. Richter).

1742-7061/$ - see front matter © 2011 Acta Materialia Inc. Published by Elsevier Ltd. All rights reserved.
doi:10.1016/j.actbio.2011.11.022

eventually necessitate implant removal; therefore, a functionalized coating for implant surfaces promoting the adhesion of human cells should not concurrently facilitate bacterial adhesion [7].

Hydrophobin DewA from *Aspergillus nidulans* is a class I hydrophobin for which large-scale production has been achieved [10]. A pilot study showed that DewA-coated surfaces provide low adhesion of human cells. The aim of this project was to investigate whether DewA could be functionalized for use on implant surfaces to prevent infection and improve tissue integration. Binding sites for integrin receptors such as the Arg–Gly–Asp (RGD) sequence of fibronectin [11,12] and the laminin globular domain LG3 [13] represent attractive cell adhesion-mediating motifs for such a functionalization. A similar approach was followed in earlier work with *Schizophyllum commune* SC3 hydrophobin, which was fused to an RGD peptide [1]. Coating with genetically engineered hydrophobin promoted growth of fibroblasts on a hydrophobic solid. In contrast to *A. nidulans* DewA, SC3 cannot be produced in *Escherichia coli* but needs to be isolated from the mushroom, a tedious and inefficient process. Application of this particular protein is consequently limited. In this project we used molecular modelling to predict suitable insertion sites for RGD or LG3 motives at surface-accessible sites in the engineered *A. nidulans* DewA molecule, and used these purified proteins to produce hydrophobin surfaces that enhance adhesion of human cells. The adhesive properties of these engineered hydrophobins were investigated for MSCs, osteoblasts, fibroblasts, chondrocytes and *S. aureus*. The effects of hydrophobins on proliferation and differentiation of MSCs were evaluated.

2. Materials and methods

2.1. Modelling of genetically modified DewA variants

In order to model the DewA domain, a motif-conserving alignment between the sequence of DewA and the class I hydrophobin EAS [14] was carried out using the Needleman–Wunsch algorithm [15]. Homology models were created using the Modeller package [16] and further relaxed in the all atom-free energy forcefield PFF02 [17] using POEM@HOME. POEM (protein optimization using energy methods) is an all atom-free energy Monte Carlo framework shown to stabilize a multitude of different protein folds; POEM@HOME is the distributed volunteer computing implementation of the POEM framework. Single simulations consist of a fixed number of Monte Carlo steps changing either single dihedral angles by a random value, or by copying favourable angles from a database of angles specific to the occurrence of two adjacent amino acids. Bond lengths are maintained during the simulation.

We modelled the *yaaD*-binding peptide domain using fragment-based modelling of the truncated *yaaD* protein fused with either one of the binding peptides (Fig. 1A). Fragments were generated using the Rosetta server [18] and assembled in the Rosetta 3.1 suite. The resulting models were then relaxed on POEM@HOME applying a protocol similar to that used in modelling of DewA.

We generated 40,000 structures each, using the standard Rosetta modelling protocol for the fusion construct of both LG3 and RGD. Each of these models was then relaxed twice independently using 500,000-step geometrical annealing Monte Carlo simulations. For 2 h run time each, these simulations consumed about 36 CPU years of simulation time. The population of structures was analysed for the accessible surface of the LG3 or RGD motifs respectively in the energy-minimized ensemble.

2.2. Insertion of peptides RGD and LG3 via primer ligation

The peptides were fused to the N-terminus of the *yaaD* via primer ligation using the RGD ligation sense AATTCATTAAAGAGGAGAAATTAACCATGCGGGGCGACCA and RGD ligation antisense CATGTGGTCGCCCCGCATGGTTAATTTCTCCTCTTTAATG, or LG3 ligation sense AATTCATTAAAGAGGAGAAATTAACCATGCCGCCGTTCCTGATGCTGCTGAAAGGTTCTACCCGTCA and LG3 ligation antisense CATGTGACGGGTAGAACCTTTCAGCAGCATCAGGAACGGCGGCATGG TTAATTTCTCCTCTTTAATG primer sets that include the sequences of the promoter region between the restriction sites *Eco*RI and *Nco*I of the vector pQE60(truncated)YaaD–DewA–His_6 [10]. The synthesized primers from MWG (Ebersberg) were purified by high-performance liquid chromatography. The primer sets were incubated in PCR-buffer at 95 °C for 1 min and then cooled down to room temperature to allow duplex formation. The vector pQE60(truncated)YaaD–DewA–His_6 [10] was digested with *Eco*RI and *Nco*I, purified from 1% agarose gels via a Zymo Gel DNA Recovery Kit (ZymoResearch, Freiburg) and ligated with the double-stranded primers overnight. The ligation mixtures were transformed into *E. coli* XL-1 Blue Cells and the correct integration was confirmed by sequencing (MWG). The vector pTT15 contains the pQE60_RGD_(truncated)YaaD–DewA–His_6 and the vector pTT18 contains the pQE60_LG3_(truncated)YaaD–DewA–His_6.

2.3. Heterologous expression and purification of peptide DewA fusion proteins by separation of the inclusion bodies (IBs)

The vectors pTT15 and pTT18 were transformed in *E. coli* Rosetta (DE3) pLysS cells. Bacterial cultures were grown overnight in EC3 medium + ampicillin. The protein expression was induced at an optical density (OD) at 600 nm of between 0.7 and 0.9, with a final concentration of 0.5 mM IPTG; cells were grown for 4–6 h at 37 °C and 225 rpm. Cells were harvested by centrifugation for 30 min at 10,000 rpm (GSA rotor).

Protein purification was performed by separation and purification of inclusion bodies (IBs). The pellet from the production culture was resuspended in 20 mM NaH_2PO_4, pH 7.5 (10 ml g^{-1} biomass). The cells were disrupted under cooling via Pressure Cell Press (American Instrument Company, 800 PSI). Subsequently, in order to separate the IBs from the cell debris and soluble proteins, cells were centrifuged 30 min in a 50 ml reaction tube at 5000 rpm, 4 °C. Cell pellets were resuspended in 20 mM NaH_2PO_4, pH 7.5 and pelleted again by centrifugation under identical conditions. Washing in 40 ml ultrapure water followed by centrifugation was repeated three times. To solubilize the IBs, the remaining pellet was resuspended in ultrapure water and mixed on a magnetic stirrer for 20 min after addition of 0.1 M NaOH. The solution was neutralized to pH 8.5–9 with 20% $H_3PO_4$and centrifuged a second time. The protein found in the supernatant was then freeze-dried.

2.4. Isolation and culture of primary human cells

The studies were approved by the local ethics committee and informed consent was obtained from all individuals included in the study. Bone marrow samples were obtained from patients undergoing total hip replacement or iliac bone graft harvest. MSCs were isolated from fresh bone marrow samples as described previously [19]. Briefly, cells were fractionated on a Ficoll-Paque Plus density gradient (GE Healthcare, Freiburg, Germany), and the low-density MSC-enriched fraction was washed and seeded at a density of 1.25×10^5 cells cm^{-2} into 0.1% gelatine-coated flasks in an expansion medium consisting of Dulbecco's modified Eagle's medium containing 4.5 mg l^{-1} glucose (DMEM-HG) (Invitrogen, Germany) with 12.5% FCS, 2 mM L-glutamine, 1% non-essential amino acids, 0.1% 2-mercaptoethanol (Invitrogen), 100 U ml^{-1} penicillin, 100 μg ml^{-1} streptomycin and 4 ng ml^{-1} human fibroblast growth factor-2 (Active Bioscience, Germany). Standard culturing conditions were used (37 °C, 6% CO_2). After 24–48 h, cultures were washed with phosphate-buffered saline (PBS) to remove non-

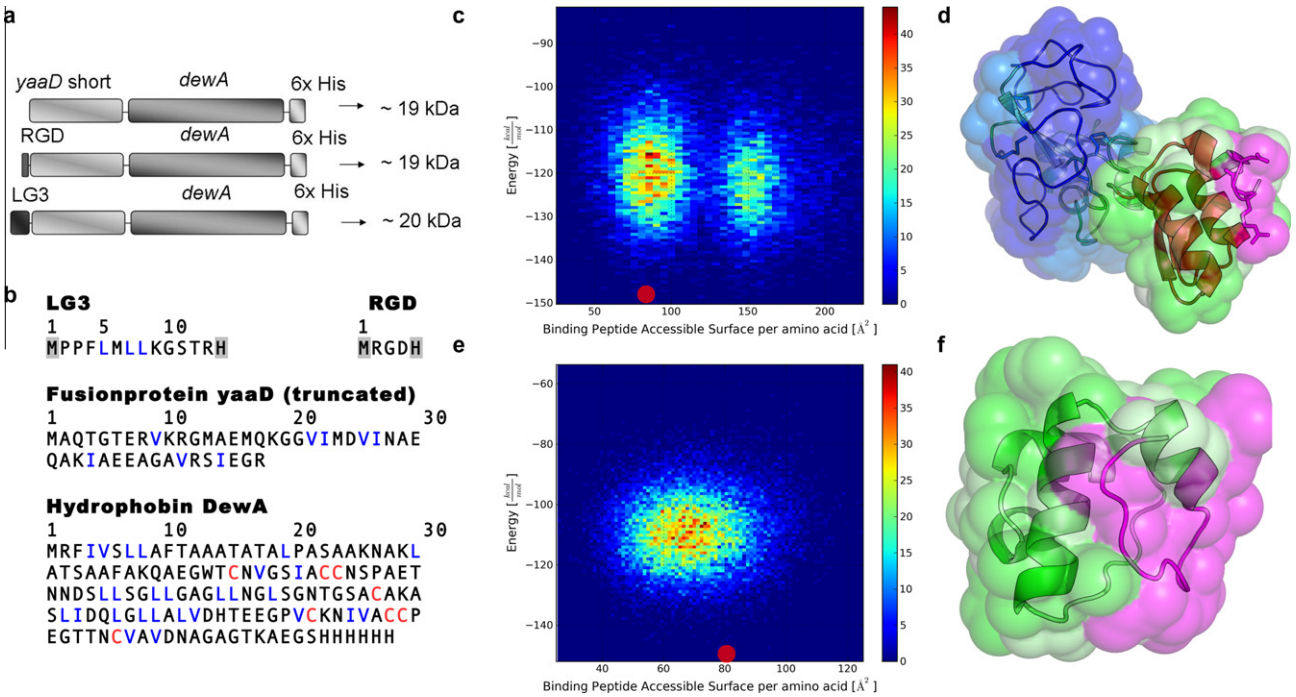

Fig. 1. Schematic representation and modelling of the DewA fusion proteins. (A) Schematic representation of the sequence of the expression constructs and masses of hydrophobin DewA with the truncated fusion protein *yaaD*, the binding motifs RGD or LG3 and a 6 × His tag. (B) Sequences of the expressed constructs. Strongly hydrophobic amino acids are highlighted in blue; the characteristic hydrophobin cystein motif is highlighted in red. Amino acids of the fusion construct linking to the RGD or LG3 motif are printed with a grey background. (C, E) Free-energy and exposed surface area per amino acids of all generated models for RGD fused with *yaaD* (MET1–ARG51) and DewA (MET52–VAL176) (C), and for LG3 fused with *yaaD* (MET1–ARG60) and DewA (MET61–VAL185) (E). The lowest energy conformations are marked with a red dot. (D) Cartoon and surface visualization of the best energy model of the full engineered protein variant fused with RGD. The model features two distinct domains: the hydrophobin domain MET52–VAL176 (light blue) and the hydrophobic loops (dark blue); and the fusion-interaction domain MET1–ARG51 (green) with the RGD (magenta). (F) Cartoon and surface visualization of the best energy model of construct LG3 (magenta) fused with *yaaD* (MET1 – ARG60, green). The DewA domain (MET61–VAL185) is not shown.

adherent material. Osteoblasts were grown from trabecular bone chips in culture medium composed of DMEM-HG containing 10% foetal calf serum (FCS; Biochrom, Berlin, Germany), 50 U ml^{-1} penicillin, 50 U l^{-1} streptomycin, 12.5 mM HEPES, 0.4 mM L-prolin, 50 mg l^{-1} ascorbic acid and 0.1 μM dexamethasone under standard conditions at 37 °C with 5% CO_2. After one passage, the medium was switched to an expansion medium consisting of DMEM-HG containing 2% FCS, with 10 ng ml^{-1} recombinant human epidermal growth factor (Strathmann Biotech, Hamburg, Germany) and 10 ng ml^{-1} recombinant human platelet-derived growth factor BB (Sigma–Aldrich, Deisenhofen, Germany) [20]. Human articular cartilage samples were obtained from patients diagnosed with osteoarthritis and undergoing total knee replacement surgery. Cartilage chips were carefully removed from the tibial plateau and condyles, and washed with PBS to avoid contamination by other cells. Human chondrocytes were isolated from cartilage by digestion with collagenase B (1.5 mg ml^{-1}) (Roche Diagnostics, Mannheim, Germany) and hyaluronidase (0.1 mg ml^{-1}) (Serva, Heidelberg, Germany), as described previously [21]. Human dermal fibroblasts were acquired from Promocell (Heidelberg, Germany). Chondrocytes and fibroblasts were expanded in the same medium as described above for osteoblasts. During expansion of all cell types, the medium was replaced two to three times each week.

2.5. Coating with hydrophobins and characterization of the surfaces by enzyme-linked immunosorbent assay (ELISA) and fluorescence microscopy

Coating of cell culture wells (96-well, Greiner, Frickenhausen, Germany) was performed with DewA, DewA–RGD or DewA–LG3 (each 200 μg ml^{-1} in water) at 4 °C. All proteins contain a 6-His tag for purification, which can also be used for immunodetection. After incubation overnight, the protein solution was removed and the surfaces blocked for 30 min (phosphate buffer solution (PBS) containing 0.1% Tween 20 and 5% milk powder). Blocking and all subsequent steps were done at room temperature. The primary antibody (anti-His antibody, GE Healthcare; diluted 1:3000 in PBS containing 0.1% Tween 20 and 1% milk powder) was applied for 1 h. After washing the wells thoroughly in PBS containing 0.1% Tween 20 four times for 5 min, the Cy3-conjugated secondary antibody (diluted 1:5000 in PBS containing 0.1% Tween 20; goat polyclonal secondary antibody to mouse IgG (Cy3), Dianova GmbH, Hamburg) was added. The wells were incubated for 1 h in the dark, washed as described above and air-dried. Next, 50 μl of PBS containing 0.1% Tween 20 was added to the wells and the samples analysed in a plate reader (Infinite® 200 PRO, Tecan, Männedorf, Switzerland). The plate reader was adjusted with the excitation wavelength of 550 nm, an emission wavelength of 570 nm and 10 flashes per well. The same wells were characterized in a fluorescent microscope at 5× magnification (AxioImagerZ.1, Software: AxioVision V4.5; Camera: AxioCam MR; Carl Zeiss, Oberkochen, Germany).

2.6. Adhesion of human cells

For the adhesion assay, culture wells (96-well plates, Greiner, Frickenhausen, Germany) were either left empty or exposed to solutions of 10 μg ml^{-1} fibronectin (Calbiochem, Darmstadt, Germany) or DewA variants (2–200 μg ml^{-1} in water) overnight at 4 °C. Wells were then washed twice with PBS. In order to block cell adhesion on possible uncoated areas, subsequent incubation with 2% bovine serum albumin (BSA; Sigma) was performed for 2 h at room temperature, followed by a washing step with PBS. This

blocking step was also performed on the uncoated wells used as negative controls.

In order to exclude variations due to cell-specific expansion, the media, MSCs, chondrocytes, osteoblasts and fibroblasts applied in adhesion assays were all expanded in the same low (2%) serum-containing medium as described above for osteoblasts. Cells expanded for three passages in this medium were trypsinized and resuspended in DMEM-HG without additives. Then 100 μl of DMEM-HG containing 10^4 cells was transferred to each well of 96-well plates in duplicate and incubated at 37 °C. After 1 h, the plates were washed with PBS using an ELISA washer (Anthos, Krefeld, Germany) to remove non-adhered cells. The remaining cells were fixed in 70% ethanol, washed and their nuclei stained with 1 μg ml^{-1} Hoechst dye (Sigma) at 37 °C. Three microscopic fields were photographed in each well (10× magnification) and the number of cells in each field was determined using the AxioVision software (Zeiss, Jena, Germany).

2.7. Proliferation assay

Ninety-six-well plates were coated as in detailed in Section 2.6. To analyse the proliferation rates on the coated surfaces, 4×10^3 MSCs per well was seeded in coated 96-well plates in triplicate. After 24 h, medium was replaced with fresh medium containing 0.25 μCi of [methyl-^{3}H]thymidine (GE Healthcare, Germany) per well. Cells were incubated for 18 h, washed and lysed in 1% Triton X-100. Half the cell lysates were transferred into tubes containing 2 ml of scintillation cocktail (Perkin Elmer, Waltham, USA). Radioactivity was measured with a WinSpectral 1414 liquid scintillation counter (Perkin Elmer, USA). The remaining cell lysates were digested overnight at 60 °C with 100 μg ml^{-1} proteinase K (Roche, Germany) in Tris–HCl, pH 8. DNA concentrations were measured with a Quant iT PicoGreen dsDNA Assay Kit (Invitrogen, Germany) according to the manufacturer's instructions.

2.8. Osteogenic differentiation and alkaline phosphatase activity assay

Twenty-four-well plates were coated as in Section 2.6: 3.5×10^4 MSCs were seeded on coated wells of 24-well plates and incubated at 37 °C. After 1 h, the plates were washed with PBS and osteogenic medium composed of DMEM-HG containing 10% FCS, 0.1 μM dexamethasone, 0.17 mM ascorbic acid 2-phosphate, 10 mM β-glycerophosphate (Sigma–Aldrich, Germany) and 1% penicillin/streptomycin was added. After 14 days, two wells each were used for assessment of alkaline phosphatase (ALP) enzyme activity. Cells were lysed with 1% Triton X-100 detergent in PBS, scraped off the plate and stored at −80 °C. ALP activity was assessed by diluting 50 μl of sample extract with 50 μl of ALP buffer (0.1 M glycine, 1 mM $MgCl_2$, 1 mM $ZnCl_2$, pH 10.4) and incubating with 100 μl of ALP buffer plus 1 mg ml^{-1} *p*-nitrophenylphosphate. The conversion to *p*-nitrophenol (*p*-NP) was measured spectrophotometrically at 405/490 nm after 1 h of incubation. The total protein concentration was determined with a Micro BCA™ Protein Assay Reagent Kit (Pierce Biotechnology, IL) according to manufacturer's instructions. The specific amount of ALP was evaluated as the amount of *p*-NP normalized with the amount of total protein.

2.9. Adipogenic differentiation

Twenty-four-well plates were coated as in Section 2.6: 3.5×10^4 MSCs in 400 μl of expansion medium were transferred on coated wells of 24-well plates and incubated at 37 °C. After 1 h, the plates were washed with PBS and adipogenic medium composed of DMEM-HG, containing 10% FCS, 0.01 mg ml^{-1} insulin, 1 μM dexamethasone, 0.2 mM indomethacin, 0.5 mM 3-isobutyl-1-methyl xanthine, 100 U ml^{-1} penicillin, and 100 mg ml^{-1} streptomycin was applied for 3 weeks. After fixation of washed cells in 4% paraformaldehyde, they were stained with 0.5% Oil Red O to visualize intracellular triglycerides (Chroma, Germany) [19]. In order to quantify lipid accumulation, Oil Red O was extracted from the cells by incubation with 60% isopropanol for 2 h at 37 °C and the OD at 490 nm was subsequently measured. Total protein concentrations, determined with the Micro BCA™ Protein Assay Reagent Kit from parallel wells, were used for normalization.

2.10. Chondrogenic differentiation and quantification of proteoglycan content

For induction of chondrogenesis at high cell density in three-dimensional culture, spheroids were formed by inclusion of a cell suspension into fibrin (Tissucol Duo STM, Baxter, Unterschleissheim, Germany) as described previously [22]. A solution containing 70–110 mg ml^{-1} fibrinogen was diluted 1:15 in PBS containing 0 or 4 μg of DewA, and a solution containing 500 IU ml^{-1} of thrombin was diluted 1:50 in PBS. Some $4–5 \times 10^5$ MSCs were suspended in 25 μl of the diluted fibrinogen solution and mixed with 25 μl of diluted thrombin solution. Medium was changed three times within the next 30 min to adjust the pH. The materials were allowed to gel at 37 °C before chondrogenic medium, consisting of DMEM-HG supplemented with 5 mg ml^{-1} insulin, 5 mg ml^{-1} tranferrin, 5 mg ml^{-1} selenous acid, 0.1 mM dexamethasone, 0.17 mM ascorbic acid-2-phosphate, 1 mM sodium pyruvate, 0.35 mM proline, 1.25 mg ml^{-1} BSA and 10 ng ml^{-1} transforming growth factor β3 (TGF β3; Sigma Aldrich), was added. Cells were kept in induction medium at 37 °C under 6% CO_2 for 42 days. After this period, spheroids were fixed and stained as described previously [23] according to standard procedures using Alcian blue (1%; Chroma, Köngen, Germany) or a monoclonal mouse anti-human collagen Type II antibody (clones I-8H5 and II-4C11, ICN Biomedicals, Aurora, Ohio, USA). For quantification of proteoglycan content, differentiated spheroids (2 per donor) were washed with PBS and mechanically crushed in 0.5 ml of guanidine hydrochloride (GuHCl) extraction buffer (4 M GuHCl/100 mM Tris, pH 8.5). After incubation (30 min, 4 °C) and centrifugation (13,000 rpm, 15 min, 4 °C), extracted proteoglycan in the supernatant was quantified with Alcian blue following Bjornsson [24]. In brief, chondroitinsulphate (3.125–200 μg ml^{-1}) was used as a standard. A 50 μl volume of SAT buffer (0.3% H_2SO_4; 0.75% Triton X-100 in aqua dist.) was added to 100 μl of supernatant before shaking for 15 min. One volume of Alcian blue stock solution (3% (w/v) Alcian blue (Roth) in 0.1% H_2SO_4, 0.4 M GuHCl) was mixed with 5 volumes of SAT buffer and 9 volumes of H_2O; 750 μl of this Alcian working solution was added. After 30 min at room temperature and shaking, the precipitate was harvested by centrifugation (15 min, 13,000 rpm, room temperature) and the supernatant rejected. The pellet was washed in 500 μl of dimethylsulphoxide buffer (40% DMSO; 0.05 M $MgCl_2$ in aqua dist.), kept at room temperature for 15 min, centrifuged (15 min, 20,000*g*) and the supernatant again rejected. In the following step, the pellet was dissolved in 500 μl of guanidine/propanol buffer (4 M GuHCl, 33% *n*-propanol; 0.25% Triton X-100). Two aliquots (200 μl) were transferred to 96-well flat-bottom plates and the absorbance was measured at 650 nm.

2.11. Adhesion of MSCs to titanium surfaces

Ti90/Al6/V4 (Goodfellow, London, UK) foil was cut into discs 13 mm in diameter using a water jet cutting system, and the discs were processed as described previously [25]. Briefly, the discs were sanded with 800, 1200 and 2500 grit silicon carbide paper, polished with colloidal silica on a ChemoMet Polishing Cloth, rinsed, sonicated twice in dichloromethane, acetone, methanol and Millipore water for 10 min each, dried in a stream of nitrogen and

stored under vacuum at 120 °C. Before use they were sonicated twice in dichloromethane, acetone, methanol and finally Millipore water for 10 min and dried in a stream of nitrogen.

Titanium discs were either left uncoated or were coated in 24-well plates under 700 μl of a solution of fibronectin (10 μg ml^{-1}) or of the DewA variants (200 μg ml^{-1}) overnight at 4 °C and washed with PBS. Discs were blocked with 2% BSA for 2 h at room temperature and washed once with 1× PBS. MSCs from four donors were expanded in Verfaille medium until passage 3. Prior to adhesion, MSCs were labelled with 100 μg ml^{-1} carboxyfluorescein succinimidyl ester (CFSE; 10 mg ml^{-1} in DMSO; Invitrogen, Molecular Probes) for 30 min, agitating at 37 °C. Cells were washed twice and resuspended in DMEM at 10^6 cells per ml. A 0.1 ml aliquot of the cell suspension was incubated on pretreated titanium discs for 1 h at 37 °C, washed using an ELISA washer (Fluido2, anthos), fixed in 70% ethanol for 20 min at 4 °C and embedded in Aquatex (Merck).

The discs were mounted on coverslips and imaged on a Zeiss Axioplan 2 microscope using the stitching function with 0% overlap and focus correction to produce a composed image of the complete titanium disc. Image analysis was performed with ImageJ version 1.43t, converting composed mosaics into 8-bit images. All images were processed equally before analysing the area fractions covered by cells. Briefly, the ImageJ "brightness and contrast" function was set to a minimum of 10 and a maximum of 50. This setting was tested in advance to subtract background signal, while permitting the detection of small single cell spots without increasing light scattering of brighter colonies. The "threshold" function was set to default algorithm in black and white mode. The settings for a lower and an upper limit were 0 and 100, respectively. The region of interest was defined as a circle with 8900 × 8900 pixels framing the chip borders. Area fractions were retrieved applying the "measure" function.

2.12. Bacterial adhesion assay

The *S. aureus* strain ATCC 49230 (American Type Culture Collection) was grown overnight on Columbia blood agar plates and subsequently inoculated into trypticase soy broth (TSB; Becton Dickinson, Cockeyville, USA). The concentration of bacteria was determined using a McFarland standard (Densimat, bioMerieux). In order to stain bacteria, 10^8 colony-forming units (CFU) in 1 ml of TSB was incubated with 10 μl of CFSE for 30 min at 31 °C. The bacteria were then washed twice by centrifugation and finally resuspended in TSB at 10^8 CFU per ml.

Titanium discs were coated as described in Section 2.11. For bacterial adhesion on one disc in one well, 1 ml of bacterial solution with 10^7 CFU of *S. aureus* in TSB was added and incubated for 1 h at 37 °C. Thereafter, the discs were washed thoroughly by dipping in PBS and fixed with 70% ethanol for 20 min. The discs were mounted on coverslips and imaged as described in Section 2.11, with settings for lower and upper cut-offs set at 0 and 40, respectively.

2.13. Statistics

Mean values and standard deviations were calculated for all variables. The non-parametric Wilcoxon test was applied for the analysis of differences in cell behaviour on different coatings. A two-tailed significance value of $p < 0.05$ was considered significant. Data analysis was performed with SPSS for Windows 16.0 (SPSS Inc., USA).

3. Results

3.1. Molecular modelling of genetically engineered DewA

In order to engineer cell-adhesive DewA surfaces, it was necessary to design genetically modified DewA variants. Among peptide sequences promoting cell adhesion, the RGD sequence (DewA–RGD) and a 12 amino acid long LG3 sequence (DewA–LG3) were selected (Fig. 1A). Structure-prediction methods were used to generate a model of proteins comprising hydrophobin, fusion construct and binding domain (Fig. 1A, D and F) to elucidate where these DewA-binding adhesion motives would be accessible on the protein surface, as potential binding partners. Analysis of the models demonstrated that the protein comprises two distinct domains (DewA–RGD: hydrophobin domain MET52–VAL176, fusion-interaction domain MET1–ARG51). The hydrophobin domain exhibited a characteristic beta-barrel structure stabilized by cysteine-bridges (CYS99–CYS165, CYS102–CYS159, CYS103–CYS135, CYS166–CYS173 for DewA–RGD) and four beta-sheets (ILE100–CYS103, CYS135–LYS137, ILE162–CYS165, CYS173–VAL176 for DewA–RGD), while the binding domains formed an unstructured conformational ensemble at the N-terminus of the fusion-protein domain. Additionally, two large unstructured hydrophobic loops were identified which give the hydrophobin its characteristic amphipathicity (SER105–SER133 and LYS137–PRO157 for DewA–RGD). Two populations of different solvent exposure of the RGD motif were identified among simulated ensembles seen in Fig. 1C. Most structures in the ensemble exhibited tightly packed helical folds for the truncated fusion protein domain and no apparent secondary structure for the RGD motif. While the lowest energy structure of the complex featured a solvent exposure of 80 $Å^2$ per amino acid of the motif, the second cluster, with a mean solvent exposure of 150 $Å^2$ per amino acid, was separated by less than 1 kcal mol^{-1}. Models from both clusters showed the RGD motif to be exposed to the solvent. Fig. 1D illustrates that the best energy model for the RGD motif lies in plane with the hydrophobic amino acids of the hydrophobin. When estimating the partition between the two populations at 120 $Å^2$ surface area per amino acid, the population of structures with a mean accessible surface of about 80 $Å^2$ comprised 9100 members, while the population with a mean accessible surface area of about 150 $Å^2$ comprised 6000 members. The overall ratio was therefore roughly 2:3. The best energy structure was found in the 80 $Å^2$ population.

A mean solvent exposure of the LG3 motif of 80 $Å^2$ per amino acid was found inside the single cluster of simulated models (Fig. 1E). Compared to the RGD structure, the LG3 motif may tend to be less exposed to the solvent in the tertiary fold. Observed tight packing of the binding peptide to the fusion domain can be explained by the large number of hydrophobic amino acids in the LG3 sequence (Fig. 1A); however, the low-energy ensemble contained many models in which a large fraction of LG3 is exposed to the solvent. Modelling showed that both DewA fusion proteins may be able to enhance cell adhesion; therefore, these proteins were synthesized and purified for subsequent testing.

3.2. Coating surfaces with DewA fusion proteins

Hydrophobin and modified hydrophobins were expressed in *E. coli* and purified as described in Materials and methods. Cell culture wells were coated with the hydrophobin-containing fraction at a concentration of 200 μg ml^{-1}, and incubated overnight at 4 °C. To ensure that comparable coatings were obtained, surfaces were characterized for the amount of bound hydrophobin using antibodies derived against the His tag of the proteins. Primary antibody detection was achieved with a Cy3-labelled secondary antibody. Fluorescence levels were quantified in a plate reader (ELISA) and suggested comparable amounts of bound protein (Fig. 2A). In addition, wells were analysed by immunofluorescence microscopy to assess spatial distribution of the proteins (Fig. 2B). Fluorescent images confirmed the ELISA data of comparable protein amounts, and also revealed that hydrophobins were

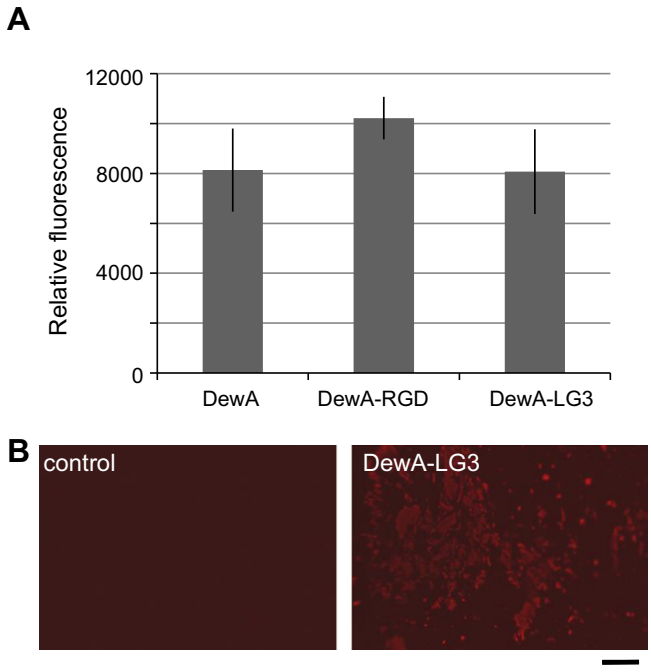

Fig. 2. Characterization of hydrophobin-coated culture wells. (A) Quantification of the relative fluorescence. For each sample the bottoms of five wells were analysed for fluorescence at five spots each in a plate reader. Excitation of Cy3 was achieved with 10 flashes. The mean value of all measurements was corrected for the value obtained in the control (PBS with Tween). (B) Immunofluorescence of the wells. Pictures of the control and the DewA–LG3 coated well were corrected for contrast and brightness using identical parameters. Pictures for DewA–RGD and DewA are not shown. Scale bar = 200 μm.

heterogeneously distributed, resulting in an unevenly coated surface.

3.3. Cell adhesion on surfaces coated with DewA fusion proteins

Adhesion of MSCs was tested on surfaces coated with DewA, DewA–RGD, DewA–LG3 and fibronectin, a common component of wound fluid which is expected to coat implants in vivo and was used as a positive control. Adhesion on laminin was analysed in preliminary experiments and showed similar levels as fibronectin for all cell types (data not shown). Both modified DewA proteins showed significantly elevated levels of MSC adhesion compared to wild-type DewA (Fig. 3A). Adhesion to DewA–RGD and DewA–LG3 remained significantly lower than with fibronectin ($p < 0.05$). At a concentration of 20 μg ml^{-1}, adhesion to DewA–RGD was significantly higher than with DewA–LG3 ($p = 0.031$).

In order to test other cell types relevant to the context of bone, adhesion of osteoblasts, chondrocytes and fibroblasts (four donors each) were quantified on surfaces coated with 200 μg ml^{-1} DewA variants. More cells from each cell type tended to adhere to DewA–RGD and DewA–LG3 than DewA, which suggests a similar pattern as with MSCs (Fig. 3B); however, the differences were not significant, possibly owing to the low number of donors (i.e. low sample size).

3.4. Proliferation of MSCs on DewA surfaces

In order to assess whether DewA-coated surfaces have cytotoxic effects, proliferation of MSCs on surfaces coated with DewA, DewA–RGD and DewA–LG3 was monitored as [^{3}H] thymidine uptake over 18 h incubation (Fig. 3C). DNA concentrations

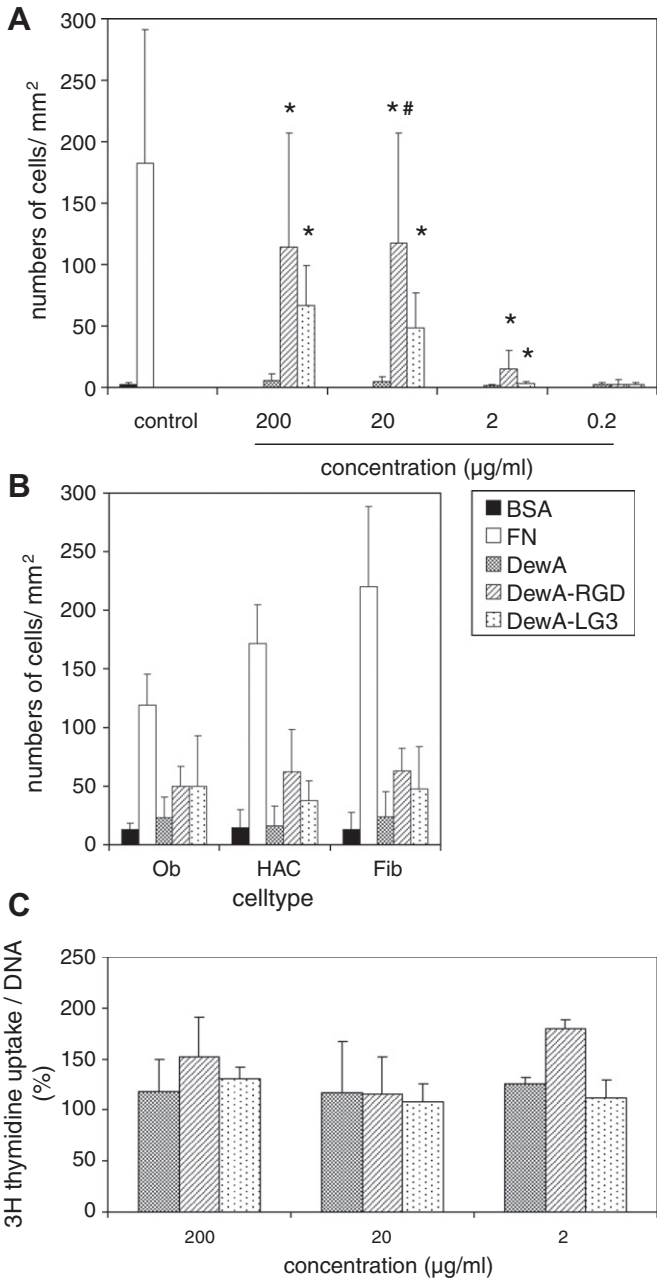

Fig. 3. Cell adhesion and proliferation on surfaces coated with DewA variants. For the quantification of cell adhesion, cells were allowed to adhere for 1 h. After fixation, the number of adherent cells per mm^2 was counted in three randomly selected photographic fields. (A) MSCs ($n = 7$ donors) were allowed to adhere to surfaces coated with BSA (2%), fibronectin (10 μg ml^{-1}) and various concentrations of the hydrophobins DewA, DewA–RGD and DewA–LG3. *Significant difference in comparison to DewA at the same concentration and to fibronectin; #significant difference in comparison to DewA–LG3 at the same concentration ($p < 0.05$). (B) Osteoblasts (Ob), chondrocytes (HAC) and fibroblasts (Fib) were allowed to adhere to surfaces coated with BSA, fibronectin and 200 μg ml^{-1} of DewA, DewA–RGD and DewA–LG3 ($n = 4$ donors for each cell type). (C0) The [^{3}H] thymidine uptake of MSCs ($n = 3$) with uncoated surfaces and on surfaces coated with DewA, DewA–RGD and DewA–LG3 were quantified and normalized with DNA content. Thymidine uptake is shown as uptake measured in MSCs on uncoated wells (%).

of cell lysates after incubation with [^{3}H] thymidine were used to normalize [^{3}H] thymidine uptake for cell numbers on the different coated surfaces. Coating with different concentrations of the DewA variants did not significantly affect proliferation of MSCs.

3.5. Differentiation of MSCs in the presence of DewA

MSCs were seeded in coated and uncoated cell culture wells, and osteogenic and adipogenic differentiation were induced. The ALP activity in MSCs after 3 weeks of in vitro osteogenesis did not differ between the uncoated surface and the surfaces coated with fibronectin or DewA variants (Fig. 4A). The adipogenic differentiation potential of MSCs was also not affected by the different coatings, which is indicated by equal levels of Oil Red O-stained intracellular triglyceride accumulation (Fig. 4B–D).

In order to evaluate a possible effect of DewA on chondrogenesis, MSCs were embedded into a fibrin gel in the presence or absence of DewA. Chondrogenic differentiation was induced by a chondrogenic medium containing 10 ng ml^{-1} TGFβ3. The immunohistochemical analysis of MSC pellets after 42 days' induction revealed similar chondrogenic differentiation with or without DewA (Fig. 4E–H). There was a trend for lower proteoglycan deposition in the presence of DewA (77% of control), but this was not significant; therefore, DewA and the variants DewA–RGD and DewA–LG3 showed no evidence of interference with the differentiation potential of MSCs.

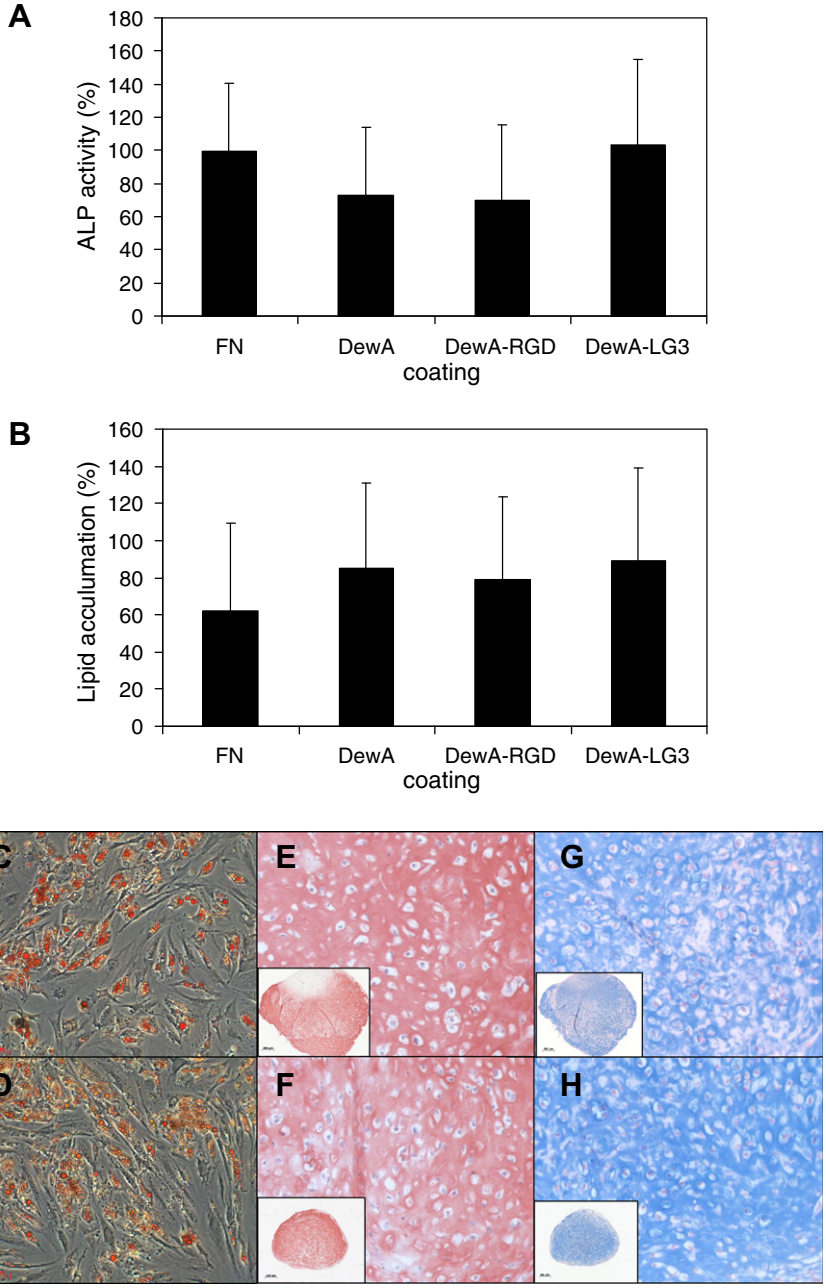

Fig. 4. Osteogenic, adipogenic and chondrogenic differentiation of MSCs in the presence of DewA. Osteogenic and adipogenic differentiation was induced in MSCs ($n = 3$) seeded on cell culture wells coated with fibronectin (10 μg ml^{-1}), DewA, DewA–RGD and DewA–LG3 (20 μg ml^{-1}) or left uncoated. All wells were blocked with BSA to cover uncoated areas. Osteogenic differentiation was quantified after 14 days by assessing alkaline phosphatase enzyme activity in cell lysates and normalized with protein concentrations. Enzyme activity is shown as a percentage of the activity of MSCs in uncoated wells (A). After 21 days of adipogenic differentiation, the Oil Red O incorporation in MSCs was quantified and expressed in relation to levels in MSCs differentiated on uncoated wells (B). A representative example of MSCs after adipogenesis on an uncoated well (C) and on a well coated with DewA (20 μg ml^{-1}) (D). Chondrogenic differentiation of MSCs ($n = 5$) was induced in pellets formed with fibrin glue only (E, G), and with fibrin glue supplemented with DewA (F, H). After 42 days, collagen Type II accumulation was evaluated by immunohistochemistry (E, F) and the accumulation of proteoglycans by Alcian blue staining (G, H). Representative pellets from one donor are shown.

3.6. Adhesion of MSCs and S. aureus to titanium surfaces

In order to test the functionality of modified DewA variants in a setting similar to the in vivo conditions in patients, titanium was used as a coating substrate. Coating was performed as previously and a similar level of adsorption as observed on the plastic wells was assumed. This hypothesis could be further analysed in future work. MSCs stained with CFSE were exposed for 1 h to coated and uncoated titanium discs. After washing, the entire surface of the titanium discs was photographed (Fig. 5A) and the percentage of the disc covered with MSCs was quantified (Fig. 5F). MSC adhesion with DewA–RGD was significantly higher compared to MSC adhesion with DewA and the negative control ($p = 0.014$ for both). For DewA–LG3, a minor but non-significant trend was observed.

Subsequently, we tested whether insertion of sequences promoting cell adhesion in DewA would modify interactions with bacteria, potentially affecting the risk of implant infection. This was achieved by quantifying the adhesion of *S. aureus* on DewA-coated titanium surfaces. Mimicking in vivo conditions in patients, an *S. aureus* strain primarily isolated from a patient with chronic osteomyelitis was used. Some 10^7 CFU of *S. aureus* stained with CFSE was exposed to titanium discs for 1 h. After washing, the entire surface of the titanium discs was photographed (Fig. 6A) and the percentage of the disc covered with bacteria was estimated (Fig. 6F). Bacterial adhesion was highest on titanium coated with fibronectin. Surfaces coated with DewA, DewA–RGD and DewA–LG3 showed similar levels of adhesion, which was significantly higher than for uncoated surfaces and significantly lower than surfaces pre-exposed to fibronectin ($p < 0.05$). DewA on titanium resulted in less bacterial adhesion than fibronectin, while the insertion of cell adhesion motifs in DewA did not increase the adhesion potential of *S. aureus* further, indicating that the bacteria, unlike other cells, did not use the RGD motif for attachment.

4. Discussion

Hydrophobins are interesting candidates for use in medical applications based on their ability to self-assemble and form thin, stable layers, as well as their apparent absence of immunogenicity and toxicity [3]; however, hydrophobins appear to be incapable of mediating mammalian cell adhesion. We have shown that adhesion of various human cell types to hydrophobin DewA is low after 1 h, and not significantly higher relative to uncoated tissue culture or titanium surfaces. Similar behaviour has been observed with the class I hydrophobin SC3, where only low numbers of fibroblasts were found after 3 days of incubation, and there was no measurable effect on proliferation [1]. Another example of this was the low numbers of rat neuronal stem cells found on surfaces coated with the hydrophobin HFBI after 24 h incubation [26]. Our data support these previous findings, showing that human cell adhesion is indeed low on surfaces coated with a class I hydrophobin.

In order to benefit from the biophysical properties of hydrophobins in applications where cell adhesion is requested, the engineering of genetically modified hydrophobins by insertion of motifs allowing cell anchoring appears to be an attractive strategy. Consequently, our construction of the two modified variants of DewA, in which the RGD [11] and the laminin globular domain LG3 [13] binding sites for integrin receptors were inserted, improved adhesion. Coatings with DewA molecules bearing one RGD or one LG3 motif allowed significantly greater adhesion compared to DewA in tissue culture wells; therefore, creating cell adhesive surfaces can be achieved with these fusion proteins.

Models of these fusion proteins exhibited a two-domain structure. Hydrophobins can be identified by a distinct sequence motif of eight cysteine amino acids, which form a very stable beta-barrel-fold structure due to four intramolecular disulphide bonds [14]. One of the domains of the fusion proteins corresponded predictably to an intact amphipathic DewA domain with a large hydrophobic patch, which may be involved in impairing cell adhe-

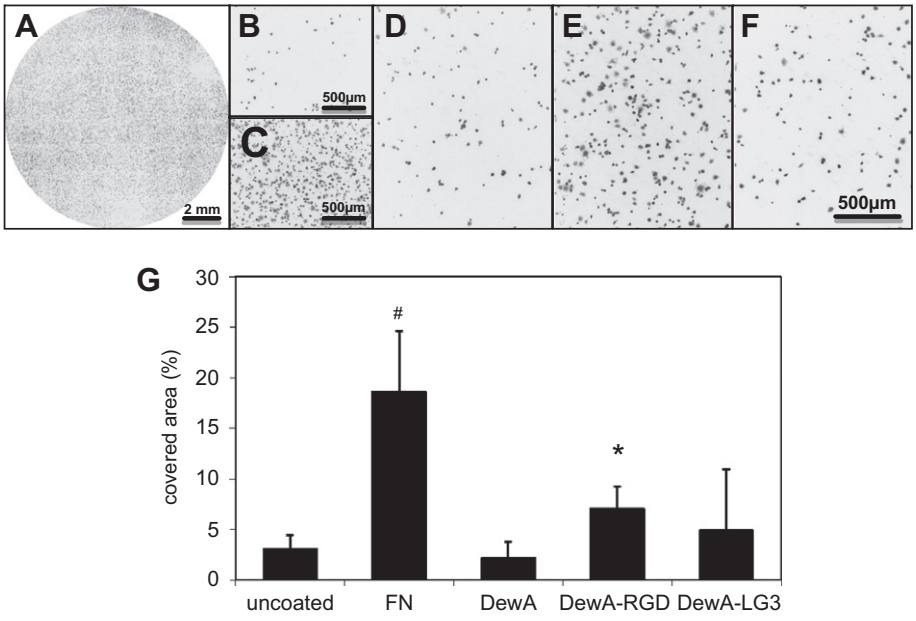

Fig. 5. Adhesion of MSCs on titanium discs coated with fibronectin and DewA variants. Fluorescent images of MSCs stained with CFSE on the coated surface of titanium discs were converted to black and white 8-bit images. An overview on a representative titanium disc coated with fibronectin (A) and detailed views on an uncoated disc (B) and discs coated with fibronectin (C), DewA (D), DewA–RGD (E) and DewA–LG3 (F). The fraction of the surface of the disc covered with MSCs was quantified using the "measure" function of ImageJ and is shown as a percentage (G). *Significantly higher than DewA and uncoated; #significantly higher than all other surfaces ($p < 0.05$).

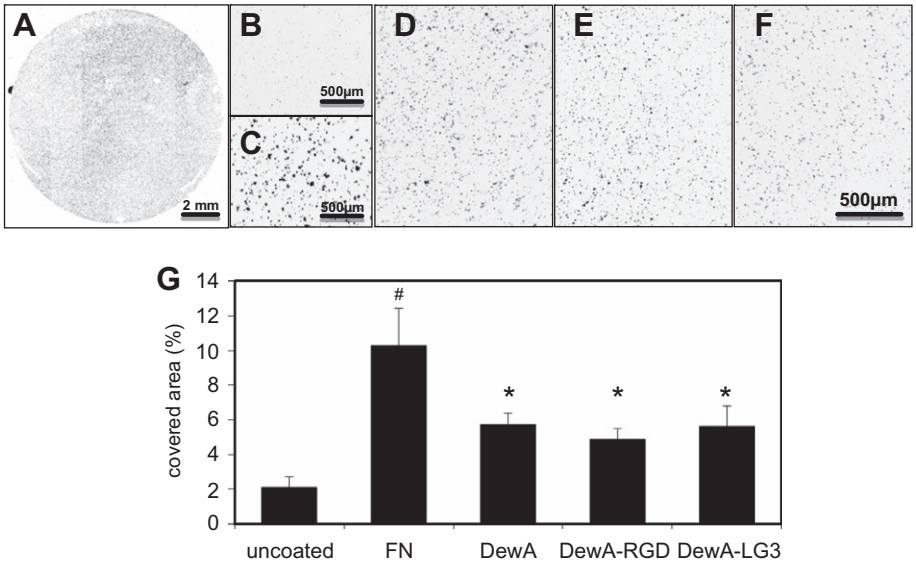

Fig. 6. Adhesion of *S. aureus* to titanium discs coated with fibronectin and DewA variants. Fluorescent images of *S. aureus* stained with CFSE on the coated surface of titanium discs were converted to black and white 8-bit images. An overview of a representative titanium disc coated with fibronectin (A) and detailed views on an uncoated disc (B) and discs coated with fibronectin (C), DewA (D), DewA–RGD (E) and DewA–LG3 (F). The fraction of the surface of the disc covered with *S. aureus* was quantified using the "measure" function of ImageJ and is shown as a percentage (G). *Significantly lower than fibronectin, significantly higher than uncoated; #significantly higher than uncoated ($p < 0.05$).

sion as seen in the experiments. Both RGD and LG3 motifs are part of the second domain, including the fusion peptide, and are found to be exposed at least partially in many of the low-energy models. The RGD motif was identified as facing the same side as the hydrophobic loops, indicating that it is exposed to area accessible by cells, which is supported by the experimentally observed increased adhesion of cells to the engineered binding-peptide mutants.

On the basis of the proposed orientation (hydrophobic loop up) of the DewA–RGD variant, we estimate an area of 13 nm^2 per protein/RGD motif or 8×10^{10} ligands per mm^2 for perfect packing, but the apparent surface density is lower. We can estimate the covered surface for a DewA–RGD covering used in the cell adhesion studies as about 20% of the total surface. This was estimated by counting the fluorescent pixels on a sample of about 1 mm^2. A similar surface density of RGD was reported by Le Saux et al. [27]. Using a variety of mirror-polished and etched silicone materials, they investigated the influence of RGD ligand density and surface roughness for endothelial cell adhesion. For an observed RGD density of 6×10^{11} ligands per mm^2, they report 700 endothelial cells mm^{-2} for a mirror-polished surface, which fell to 300 cells mm^{-2} for a silicone surface etched for 10 min. Adherent endothelial cells featured a mean cell surface of 400 μm^2. The cells used in this investigation featured a surface area of roughly 700–1000 μm^2. Our investigations were done in cell culture wells of unknown roughness; however, the number of cells for the fibronectin positive control is comparable to the etched silicone (300 vs. 180 cells mm^{-2}), considering the increased surface area of the stem cells. The efficiency of 60% of the RGD-modified hydrophobin construct in comparison to the fibronectin-positive control can be explained by the unordered surface coverage of 20%. An expected efficiency of 20% is incorrect, as shown by Le Saux et al. [27]. They showed that a decreased RGD ligand density can actually lead to increased endothelial cell binding. Our sample showed unordered ligand densities; therefore a lower efficiency is to be expected.

Furthermore, it should be noted that surface coating with DewA was heterogeneous in this study. Whereas the *A. nidulans* hydrophobin RodA is able to form rodlets on the spore surface, DewA does not have this ability [28,29]. Rodlet formation on artificial surfaces has not yet been observed for either DewA (Fig. 2B) or RodA (unpublished data). More homogeneous surfaces can be obtained at higher temperatures, as was discovered in an independent project [30]; however, as the amount of each DewA variant on the cell culture wells was the same, this heterogeneity did not interfere with the differences observed between them.

The RGD cell attachment site has been described well, and it allows cell adhesion that can be mediated through about half of the existing integrin receptors [12]. Adhesion to the globular domain of laminin has been shown to be mediated by the 12 amino acid motif PPFLMLLKGSTR [13]. Adhesion to this domain is mediated by the integrin $\alpha 3\beta 1$, as has been shown for human keratinocytes [13] and MSCs [31]. As integrin $\alpha 3\beta 1$ does not play an important role in adhesion to RGD motifs [32,33], adhesion to the modified DewA variants bearing the RGD and LG3 motif is likely mediated by different integrins. Relatively low adhesion on DewA–LG3 could be attributable either to a less exposed conformation of the fusion protein or to differential adhesion potentials of cells to RGD and LG3. However, as a further development, our results raise the possibility of creating DewA surfaces that target different cell adhesion receptors, which could allow selective adhesion of specific cell types.

Proliferation of MSCs on DewA surfaces was not altered in comparison to fibronectin or uncoated cell culture wells. This is in line with studies of other hydrophobins showing the absence of cytotoxicity [1,26]. Nonetheless, the differentiation potential of MSCs in contact with hydrophobins has not previously been analysed. Our study demonstrated that DewA does not affect the differentiation potential of MSCs towards the osteogenic, adipogenic and chondrogenic lineage. Moreover, DewA fusion proteins including RGD and LG3 did not modify the potential of MSCs for osteogenic and adipogenic differentiation. The differences in cell adhesion of these molecules, in comparison to fibronectin, did not appear to be relevant to the differentiation of MSCs over several weeks. Studies have reported a stimulatory effect of RGD and a larger sequence from the LG3 domain on osteogenic differentiation in experimental settings that differed substantially from ours [31,34]. Under the conditions used in our study, such an effect was not observed;

however, hydrophobins could permit the design of surfaces with osteoinductive properties, for example by combining DewA–RGD or DewA–LG3 coatings with DewA proteins fused to modular peptides that promote osteogenic differentiation [35].

Infections of prosthetic implants represent a serious complication with potentially devastating consequences [9]. Bacterial adhesion represents the first step leading to the formation of biofilms, which are crucial for the virulence of the infection. Adhesion of *S. epidermis* on fibronectin has been extensively analysed and has been shown to correlate to the potential for biofilm formation on fibronectin [36]. Until now, the interaction of hydrophobins with bacteria typically implicated in nosocomial infections has not been investigated. Although we found a higher adhesion of *S. aureus* to titanium coated with DewA than on uncoated titanium, bacterial adhesion to DewA was significantly lower than with fibronectin, a common component of wound fluid. This finding suggests that our adhesion assay of surfaces coated with DewA, DewA–RGD or DewA–LG3 equally induce lower bacterial adhesion than fibronectin, which may form a coating on the titanium immediately post-implantation. Even more importantly, bacterial adhesion was not enhanced by the insertion of motifs that allow anchoring of human cells, which agrees with the hypothesis that, relative to other cells, bacteria uses an alternative form of attachment. This indicates that our insertion of the RGD motif to encourage adhesion to human cells would not increase the risk of infectious bacteria attaching to these surfaces. Overall, DewA–RGD thus appears to be an attractive coating to produce surfaces with enhanced human cell adhesion, but which do not support bacterial biofilm formation.

5. Conclusions

We have shown that a scalable synthesis of hydrophobins bearing motifs encouraging anchoring of human cells is possible, and these hydrophobins can be used to produce surfaces enhancing the adhesion of human cells such as MSCs, osteoblasts, fibroblasts and chondrocytes. Furthermore, these modified hydrophobins did not interfere with the functionality of MSCs. The enhanced cell adhesion on surfaces coated with the modified hydrophobins DewA–RGD and DewA–LG3 could therefore be coupled to proliferation and differentiation of MSCs on these surfaces, allowing good integration of the coated surface with the neighbouring tissue. Improved cell adhesion potential of human cells on these surfaces was not coupled with enhanced bacterial adhesion and therefore does not introduce increased risk of bacterial infection.

Acknowledgements

This work was supported by a grant from the Landesstiftung Baden-Württemberg (P-LS-Biomat/31). The authors would like to thank Dr. C. Bollschweiler, BASF SE, for support and advice for production of the hydrophobins, Prof. Maike Stiesch for providing titanium discs and Simone Gantz for statistical support.

Appendix A. Figures with essential colour discrimination

Certain figures in this article, particularly Figs. 1, 2 and 4, are difficult to interpret in black and white. The full colour images can be found in the on-line version, at doi:10.1016/j.actbio.2011.11.022.

References

[1] Janssen MI, van Leeuwen MB, Scholtmeijer K, van Kooten TG, Dijkhuizen L, Wosten HA. Coating with genetic engineered hydrophobin promotes growth of fibroblasts on a hydrophobic solid. Biomaterials 2002;23:4847–54.
[2] Gebbink MF, Claessen D, Bouma B, Dijkhuizen L, Wosten HA. Amyloids – a functional coat for microorganisms. Nat Rev Microbiol 2005;3:333–41.
[3] Scholtmeijer K, Wessels JG, Wosten HA. Fungal hydrophobins in medical and technical applications. Appl Microbiol Biotechnol 2001;56:1–8.
[4] Wösten HA. Hydrophobins: multipurpose proteins. Annu Rev Microbiol 2001;55:625–46.
[5] van Wetter MA, Wösten HA, Wessels JG. SC3 and SC4 hydrophobins have distinct roles in formation of aerial structures in dikaryons of *Schizophyllum commune*. Mol Microbiol 2000;36:201–10.
[6] Aimanianda V, Bayry J, Bozza S, Kniemeyer O, Perruccio K, Elluru SR, et al. Surface hydrophobin prevents immune recognition of airborne fungal spores. Nature 2009;460:1117–21.
[7] Groll J, Fiedler J, Bruellhoff K, Moeller M, Brenner RE. Novel surface coatings modulating eukaryotic cell adhesion and preventing implant infection. Int J Artif Organs 2009;32:655–62.
[8] Boeuf S, Richter W. Chondrogenesis of mesenchymal stem cells: role of tissue source and inducing factors. Stem Cell Res Ther 2010;1:31.
[9] Trampuz A, Widmer AF. Infections associated with orthopedic implants. Curr Opin Infect Dis 2006;19:349–56.
[10] Wohlleben W, Subkowski T, Bollschweiler C, von Vacano B, Liu Y, Schrepp W, et al. Recombinantly produced hydrophobins from fungal analogues as highly surface-active performance proteins. Eur Biophys J 2010;39:457–68.
[11] Ruoslahti E, Pierschbacher MD. New perspectives in cell adhesion: RGD and integrins. Science 1987;238:491–7.
[12] Hersel U, Dahmen C, Kessler H. RGD modified polymers: biomaterials for stimulated cell adhesion and beyond. Biomaterials 2003;24:4385–415.
[13] Kim JM, Park WH, Min BM. The PPFLMLLKGSTR motif in globular domain 3 of the human laminin-5 alpha3 chain is crucial for integrin alpha3beta1 binding and cell adhesion. Exp Cell Res 2005;304:317–27.
[14] Kwan AH, Winefield RD, Sunde M, Matthews JM, Haverkamp RG, Templeton MD, et al. Structural basis for rodlet assembly in fungal hydrophobins. Proc Natl Acad Sci U S A 2006;103:3621–6.
[15] Needleman SB, Wunsch CD. A general method applicable to the search for similarities in the amino acid sequence of two proteins. J Mol Biol 1970;48:443–53.
[16] Eswar N. Comparative Protein Structure Modeling Using MODELLER. New York: John Wiley & Sons; 2001.
[17] Verma A, Wenzel W. A free-energy approach for all-atom protein simulation. Biophys J 2009;96:3483–94.
[18] Raman S, Vernon R, Thompson J, Tyka M, Sadreyev R, Pei J, et al. Structure prediction for CASP8 with all-atom refinement using Rosetta. Proteins 2009;77(Suppl 9):89–99.
[19] Winter A, Breit S, Parsch D, Benz K, Steck E, Hauner H, et al. Cartilage-like gene expression in differentiated human stem cell spheroids: a comparison of bone marrow-derived and adipose tissue-derived stromal cells. Arthritis Rheum 2003;48:418–29.
[20] Reyes M, Lund T, Lenvik T, Aguiar D, Koodie L, Verfaillie CM. Purification and ex vivo expansion of postnatal human marrow mesodermal progenitor cells. Blood 2001;98:2615–25.
[21] Benz K, Breit S, Lukoschek M, Mau H, Richter W. Molecular analysis of expansion, differentiation, and growth factor treatment of human chondrocytes identifies differentiation markers and growth-related genes. Biochem Biophys Res Commun 2002;293:284–92.
[22] Dickhut A, Gottwald E, Steck E, Heisel C, Richter W. Chondrogenesis of mesenchymal stem cells in gel-like biomaterials in vitro und in vivo. Front Biosci 2008;13:4517–28.
[23] Pelttari K, Winter A, Steck E, Goetzke K, Hennig T, Ochs BG, et al. Premature induction of hypertrophy during in vitro chondrogenesis of human mesenchymal stem cells correlates with calcification and vascular invasion after ectopic transplantation in SCID mice. Arthritis Rheum 2006;54:3254–66.
[24] Bjornsson S. Simultaneous preparation and quantitation of proteoglycans by precipitation with alcian blue. Anal Biochem 1993;210:282–91.
[25] Heuer W, Winkel A, Kohorst P, Lutzke A, Pfaffenroth C, Menzel H, et al. Assessment of the cytocompatibility of poly-(*N*-hexylvinylpyridinium) used as an antibacterial implant coating. Adv Eng Mater 2011;12:B609–17.
[26] Li X, Hou S, Feng X, Yu Y, Ma J, Li L. Patterning of neural stem cells on poly(lactic-co-glycolic acid) film modified by hydrophobin. Colloids Surf B Biointerfaces 2009;74:370–4.
[27] Le Saux G, Magenau A, Böcking T, Gaus K, Gooding JJ. The relative importance of topography and RGD ligand density for endothelial cell adhesion. PLoS ONE 2011;6:e21869.
[28] Stringer MA, Dean RA, Sewall TC, Timberlake WE. Rodletless, a new *Aspergillus* developmental mutant induced by directed gene inactivation. Genes Dev 1991;5:1161–71.
[29] Stringer MA, Timberlake WE. DewA encodes a fungal hydrophobin component of the Aspergillus spore wall. Mol Microbiol 1995;16:33–44.
[30] Rieder A, Ladnorg T, Wöll C, Obst U, Fischer R, Schwartz T. The impact of recombinant fusion-hydrophobin coated surfaces on E. coli and natural mixed culture biofilm formation. Biofouling 2011;27:1073–85.
[31] Klees RF, Salasznyk RM, Ward DF, Crone DE, Williams WA, Harris MP, et al. Dissection of the osteogenic effects of laminin-332 utilizing specific LG domains: LG3 induces osteogenic differentiation, but not mineralization. Exp Cell Res 2008;314:763–73.

[32] Wu C, Chung AE, McDonald JA. A novel role for alpha 3 beta 1 integrins in extracellular matrix assembly. J Cell Sci 1995;108:2511–23.
[33] Ruoslahti E. RGD and other recognition sequences for integrins. Annu Rev Cell Dev Biol 1996;12:697–715.
[34] Taubenberger AV, Woodruff MA, Bai H, Muller DJ, Hutmacher DW. The effect of unlocking RGD-motifs in collagen I on pre-osteoblast adhesion and differentiation. Biomaterials 2010;31:2827–35.
[35] Lee JS, Lee JS, Murphy WL. Modular peptides promote human mesenchymal stem cell differentiation on biomaterial surfaces. Acta Biomater 2010;6:21–8.
[36] Christner M, Franke GC, Schommer NN, Wendt U, Wegert K, Pehle P, et al. The giant extracellular matrix-binding protein of Staphylococcus epidermidis mediates biofilm accumulation and attachment to fibronectin. Mol Microbiol 2010;75:187–207.